Iranian Journal of Catalysis 10(3), 2020, 181-188

IRANIAN JOURNAL OF CATALYSIS

Green synthesis of iron nanoparticles by *Terminalia arjuna* bark extract and photodegradation of rose bengal

Mrunal Vishnu Kangralkar, Jayappa Manjanna*

Department of Chemistry, Rani Channamma University, Belagavi 591156, Karnataka, India.

Received 19 January 2020; received in revised form 28 July 2020; accepted 3 August 2020

ABSTRACT

In this study, iron nanoparticles (FeNPs) were synthesized by green route under microwave irradiation. *Terminalia arjuna* bark extract was used for synthesis, which acts as reducing and stabilizing agent. The synthesized FeNPs were characterised by UV-Visible spectra, X-ray diffraction (XRD), scanning electron microscopy (SEM), Fourier transform infrared spectra (FT-IR), BET surface area and UV-DRS (diffuse reflectance spectrophotometer). The absorption spectra of FeNPs showed a surface plasmon resonance (SPR) peak at 280 nm. The photocatalytic activity of rose bengal by FeNPs was studied under sunlight and UV light (250 W) of photocatalytic reactor. The percentage of photodegradation of RB was 83 % and 95 %, in about 240 min and 200 min in sunlight and UV light, respectively. The photocatalytic degradation of RB by Fe NPs follows pseudo-first order kinetics. The photodegradation of RB was confirmed by LC-MS analysis.

***Keywords**: Iron nanoparticles, Terminalia arjuna bark extract, Rose bengal, Photodegradation.*

1. Introduction

Nanotechnology is used in various fields such as medical science, physics, engineering, chemistry, biology etc [1]. Metal and metal oxide nanoparticles are used for remediation of wastewater and wastewater pollutants. Metal nanoparticles like Fe (iron), Cu (copper), and Ag (silver) have great advantage in remediation of organic pollutants, dyes, and heavy metals from contaminated water [2-4]. Nanoparticles offer better properties because of their reduced size, huge specific surface area, surface active sites and efficient reactivity [5].

Different methods are reported for nanoparticle synthesis, but synthesis by green route eliminates the formation of by products, which are harmful to human being and environment. By use of plant extract, it will easy to synthesize nanoparticles in short time, cheaply and even eco-friendly to environment [6]. Biomolecules like polyphenols, flavonoids, proteins, tannins, saponins [1], polyols, terpenoids, organic acids present in plant, manage the composition, phase, direction and geography of inorganic salts, causing formation of nanosized particles [7].

*Corresponding author.
E-mail address: jmanjanna@rediffmail.com (**J. Manjanna**)

FeNPs synthesis by green route using plant extract such as *Psidium gujava* [8], *Rosa damascene*, *Thymus vulgaris*, *Urtica dioica* [9], Eucalyptus leaf extract [10], green tea extract [2] etc have been reported.

Mostly coloured dyes are used in textile, paper, cosmetics, pharmaceutical, food industries [11-14]. These dyes in the form of cationic, anionic, and neutral dye effluents from industries mixed with water thereby physical and chemical nature of water gets damaged. Most of these dyes are synthetic and aromatic in nature. Aromatic dyes are stable and difficult to remove [15]. Approximately 15% of dye stuff is emitted through industrial effluents. It is estimated that for 1 Kg of industry product, about 100 L of wastewater is produced, which causes chronic diseases to living organisms [16]. A dye molecule in wastewater causes carcinogenicity, mutagenicity and toxicity thereby mostly delicate body organs and systems of body can be damaged in human beings [17-19]. Among the number of dyes, rose bengal (RB) is a xanthenes dye used in textile and photochemical industries [20]. It is halogenated triarylmethane dye [21]. Molecular formula of RB is $C_{20}H_4Cl_4I_4O_5$ (1017.63 g/mol). IUPAC name of RB is disodium 2,3,4,5-tetrachloro-6-(2,4,5,7-tetraiodo-3-oxido-6-oxoxanthen-9-yl) benzoate. It is mildly toxic

bright red stain, effects on epithelial cells, mucus, and fibrous tissues. So, its removal from aqueous media is important. Photodegradation is one of the best techniques for destruction of dyes from wastewater.

In photocatalysis, catalyst increases the rate of photoreaction in optimum condition. As day by day environmental problems increasing and semiconductor photocatalysts have huge role in energy applications, they are used in adsorption, degradation of dyes and organic pollutants [19, 22-24], hydrogen generation in visible light [25], electronic induced CO_2 dissociation [26] etc. In catalysed photolysis, the light energy must be same or higher than the semiconductors band gap energy, is absorbed by an adsorbed substrate and create electron-hole pairs on the catalyst surface. The holes h^+ (h^+_{VB}) oxidizes H_2O or OH^- to yield $HO^\bullet$ and anionic superoxide radical ($O_2^{-\bullet}$) formed by the electron ($e^-_{(CB)}$) These $^\bullet OH$, H_2O_2 and $O_2^{-\bullet}$ species are responsible for degradation of dyes [3, 26-28]. FeNPs are used for degradation of bromothymol blue [2], methyl orange, sunset yellow and acid blue [29], lindane [30], methylene blue and methyl orange [31] and even for removal of heavy metal like chromium [6] etc.

Use of microwave oven decreases the preparation time and energy consumption and high yield of product/s than chemical methods. Thus, biosynthetic method with microwave usage improves the NPs synthesis through green chemistry conditions. Microwave assisted synthesis of metal/metal oxide nanoparticles by extract of plants is a rapid and simple method [32, 33]. Microwave irradiation provides rapid formation of FeNPs with larger surface area compared to conventional chemical methods. We reported here microwave irradiated biosynthesis of iron nanoparticles through ferrous nitrate and *Terminalia arjuna* bark extract. Extract of T. arjuna bark acts as reducing and capping agent in iron nanoparticle (FeNPs) synthesis and these FeNPs were used here for the photodegradation of rose bengal in aqueous medium.

2. Experimental

2.1. Reagent and materials

Dry bark of *Terminalia arjuna* plant was collected from Belagavi (Karnataka, India) ferrous nitrate ($Fe(NO_3)_2$ $9H_2O$), rose bengal dye were used without further purification. Distilled water and analytically grade chemicals were used in whole experiments. Microwave oven and photochemical reactor were used for irradiation of reaction mixture and degradation of rose bengal, respectively.

2.2. Preparation of FeNPs

Approximately 10 g dried pieces of *T. arjuna* bark was taken into tiny pieces, then washed 2-3 times with distilled water to eliminate any adsorbed contamination on the surface of bark. Then it was transferred to 100 mL distilled water, in RB flask and treated for microwave irradiation at constant power of 300 W for microwave exposure time about 5-7 min to remove phyto-constituents of *T. arjuna* bark. In microwave, reaction is fast as due to uniform heating which causes homogeneous nucleation and growth of metal/metal oxide nanoparticles. 2.45 GHz frequency radiations are generated by interaction of permanent dipole moment molecule. Thus reaction is reduced by a factor ~ 20 as compared to usual heating [34]. Through 0.2 µm membrane hot *T.* arjuna bark extract filtered to get free from fibrous contamination. 10 mL of this stock solution was placed in 10-2 (50 mL) ferrous nitrate solution. The yellow colour changed to greenish black. The reaction mixture was irradiated in microwave oven for different time where the mixture colour changed to black after 5 min and spectra of mixture was recorded by UV-Vis absorption spectrophotometer. $Fe^{2+} \rightarrow Fe^0$ reduction took place in 5 min in microwave oven. The FeNPs here were black in colour showing an absorption maximum around 280 nm. Finally, the irradiated mixture was centrifuged, washed with distilled water and dried at 70 °C to get FeNPs in powdered form.

Fig. 1 shows the schematic representation of the formation of FeNPs using the precursor ferrous nitrate and extract of *T. arjuna* bark in microwave oven.

2.3. Photolytic experiments

Photochemical reactor contain glass made double jacket cylinder of 1L capacity. Outer jacket is used to circulate water around the inner jacket and in inner jacket, UV lamp (250 W) was inserted. The UV lamp was 3 mm apart from the solution glass cylinder.

100 mg FeNPs were dispersed in 1000 mL RB stock solution for UV irradiation in photochemical reactor as well as open sunlight to different interval of time.

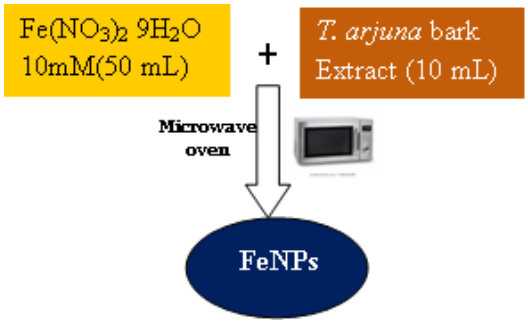

Fig. 1. Schematic representation of FeNPs preparation.

Prior to photocatalytic activity, both suspensions, sunlight and photocatalytic reactor were kept for 30 min in dark to attend adsorption/desorption equilibrium. Absorption band (λ_{max}) of initial RB solution was at about 545 nm recorded by using UV-Vis spectrophotometer.

Suspensions of 20 ppm RB (1000 mL) and 100 mg of FeNPs in beaker was taken and covered by plastic paper and kept in sunlight for about 240 min (from 12 noon to 4 pm in April 2018). Similarly, suspension of 5 ppm RB solution (1000 mL) and 100 mg of FeNPs was taken in photochemical reactor with magnetic stirrer. For both the experiments, solid-to-liquid ratio was 1:10 for FeNPs (mg) and RB solution (mL) respectively.

After regular interval of period, 5 mL of suspension was filtered through syringe filter to eliminate FeNPs particles and UV-Vis spectra was monitored. Photodegradation rate for each experiment was calculated by using equation 1.

$$Photodegradtion\ (\%) = \frac{(C_i - C_f)\times 100}{C_i} \qquad (1)$$

where C_i and C_f are initial and final concentrations of RB solution, respectively.

3. Results and discussion

3.1. Characterizations

Prepared FeNPs were analysed by UV-Visible spectrophotometer, XRD, FT-IR and BET specific surface area. FE-SEM image was recorded for morphology of FeNPs.

3.1.1. UV-Vis spectrophotometer

Fig. 2 and inset shows UV-Visible spectra of T. *arjuna* bark extract – A, 10 mM ferrous nitrate – B and mixture –C from microwave to 5 min (A+B) respectively.

Fig. 3 shows UV-Vis spectra of FeNPs to different period. The reduction of ferrous nitrate solution was seen from the colour change from yellow to black. Absorbance increased with increase in reaction time. $Fe^{2+} \rightarrow Fe^0$ reduction takes place, as biomolecules act reducing agent present in *T. arjuna* bark extract. Absorption peak of synthesized FeNPs was at 280 nm because of surface plasmon resonance (SPR) effect [35-36]. SPR peak of FeNPs was observed at 293 nm [37] and 235 nm [38].

3.1.2. FT-IR analysis

Fig. 4 shows FT-IR spectra of FeNPs. The extract of *T.* arjuna bark contains polyphenols, flavonoid, glycosides, triterpenoids, saponins, tannins etc is reported in ref [39-41].

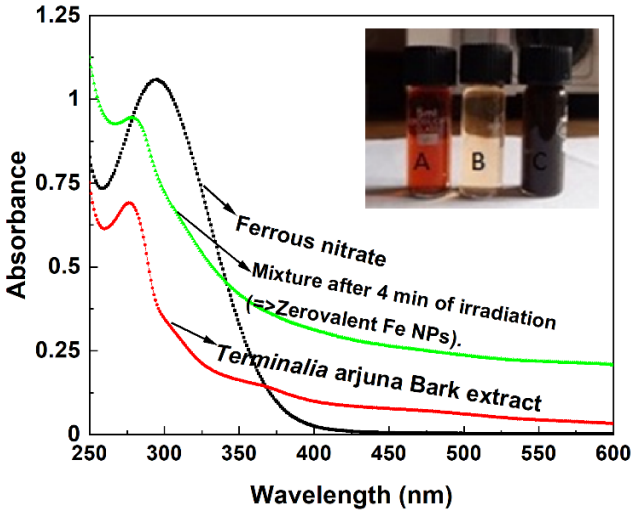

Fig. 2. UV-Visible spectra of *T. arjuna* bark extract, ferrous nitrate and the reaction mixture after ~ 5 min of microwave irradiation. Inset shows extract of *T. arjuna* bark (A), 10 mM ferrous nitrate (B) and mixture of both (C).

Polyphenols in plant extract were responsible for the preparation of nanoscale Fe^0 particles with unique properties [5]. Absorption intensity band at 3452 cm^{-1} is due to O-H stretching vibrations i.e. polyphenol compounds causes reduction of Fe^{2+} to Fe^0. The band at 1634 cm^{-1} is due to aromatic stretching vibrations of C=C and 1384 cm^{-1} is for CH_3 asymmetric stretching [42-43]. FeNPs synthesis through plant extracts may be represented as [10, 44-45]

$nFe^{2+} + 2Ar\text{-}(OH)_n \rightarrow nFe^0 + 2nAr{=}O{+}2nH^+$ where Ar is phenyl group and n is the number of hydroxyl groups oxidized by Fe^{2+}. In this study, the FeNPs formed are stable due to the presence of capping agents.

Fig. 5 shows the XRD pattern of as obtained FeNPs. The poor nature of XRD diffraction peak was due to amorphous nature of FeNPs particles.

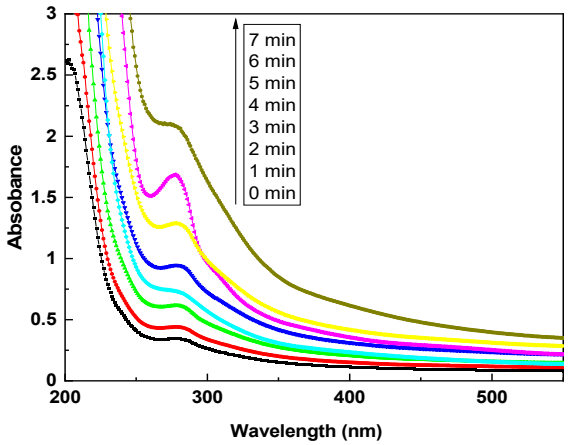

Fig. 3. UV-Visible spectra of FeNPs during the irradiation of reaction mixture.

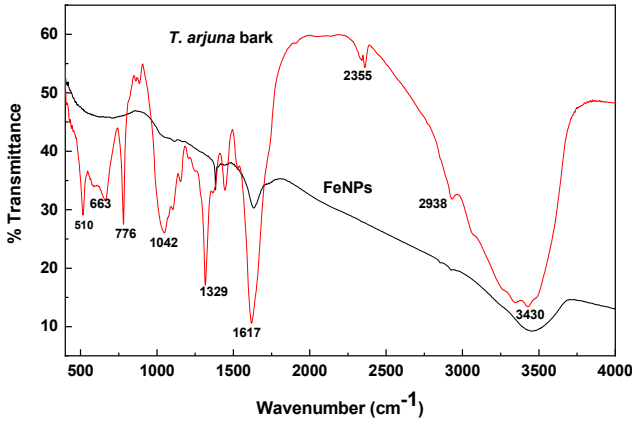

Fig. 4. FT-IR spectra of Terminalia arjuna bark (fine powder) and FeNPs.

3.1.3. XRD analysis

In XRD of FeNPs, a broad peak around 2θ = 25^0 ascribed to lattice plane (200) because of organic matter from the bark extract, which act as capping and reducing agent [46-47]. For zero-valent FeNPs, 2θ peak was observed at 44.75° [38]. In our sample, the peak at 25^0 is due to polyphenol compounds from plant extract present on the amorphous FeNPs [48]. Although the FeNPs obtained here are dried at 70 ^{0}C, there was no improvement in the crystallinity.

3.1.4. FE-SEM analysis

The surface morphology of FeNPs is evident from SEM image as shown in Fig. 6. The structure is relatively uniform and globular in nature causing large surface area with diameter between 20-80 nm. Polyphenols in *T. arjuna bark* extract act as capping agent, to manage aggregation and dispersion improvement of FeNPs.

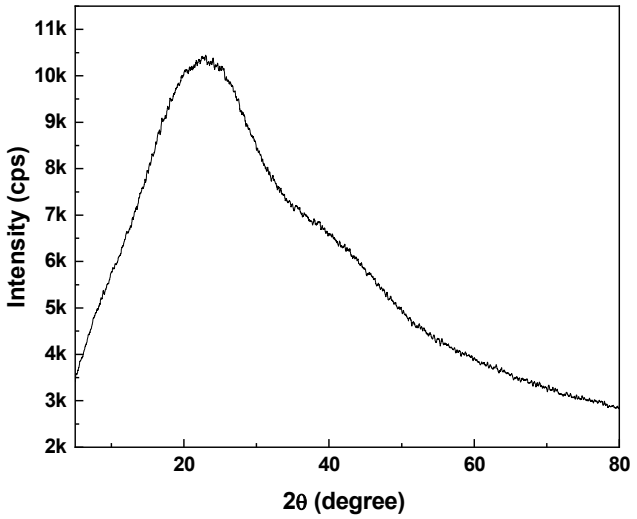

Fig. 5. Powder XRD pattern of FeNPs (after heating to 70 °C).

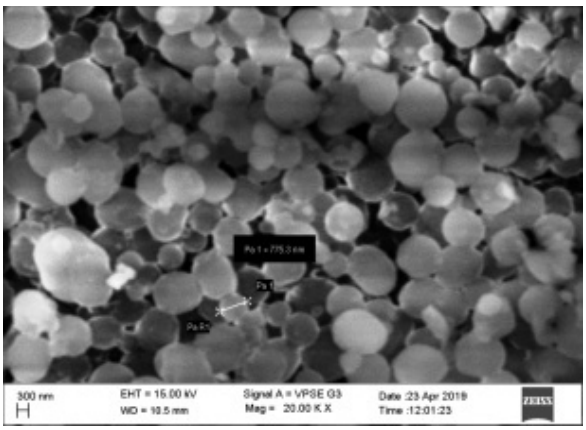

Fig. 6. FE-SEM image of FeNPs.

3.1.5. UV-DRS and BET analysis

The DR UV-Vis spectra of FeNPs is given in Fig. 7a, which shows a peak around 290 nm. The sharp peak indicates FeNPs are in zero-valent state. The peak intensities decrease and broader because of decreasing in particle size. The DRS of FeNPs was calculated by using Kubelka-Munk equation, $K = (1-R)^2/2R$ where K is the transformed reflectance and R is the reflectance (in %) obtained in DRS [49-50].

BET N_2 adsorption/desorption isotherm of FeNPs was shown in Fig. 7b. BET-BJH test, the specific surface area of FeNPs by this test was relatively small, around 4.18 $m^2\ g^{-1}$ and pore volume were about 7×10^{-3} cm^3g^{-1}. Fazlzadeh et al. (2017) reported specific surface area for iron nanoparticles for three plant extracts viz., *Rosa damascene*, *Thymus vulgaris* and *Utrica dioica* as 1.42, 1.63 and 2.42 m^2g^{-1}, respectively [9] and Bagbi et al. (2017) have reported 4.4 m^2g^{-1} [51].

3.2. Photodegradation of RB

RB dye without FeNPs shows negligible degradation (< 5%) in presence of sunlight and photocatalytic reactor. UV-Vis spectra of suspensions in sunlight and photocatalytic reactor at different period interval was as shown in Fig. 8a and Fig. 9a, respectively. As irradiation time increases, there was decrease in absorption intensity of RB and nearly entire photodegradation of RB took place. The RB degradation in presence of sunlight is 83 % (240 min) whereas in UV light it is 95 % (200 min) as shown in Fig. 8a and Fig. 9a respectively.

Fig. 10 gives the kinetic data of photodegradation under sunlight, UV light and in absence of FeNPs. Photodegradation of RB by FeNPs follows pseudo-first order kinetics as given in Fig. 11. It is expressed as, $\ln(C_0/C_t) = kt$, where C_0 initial concentration and C_t concentration at time t (min), k is pseudo-first order rate constant.

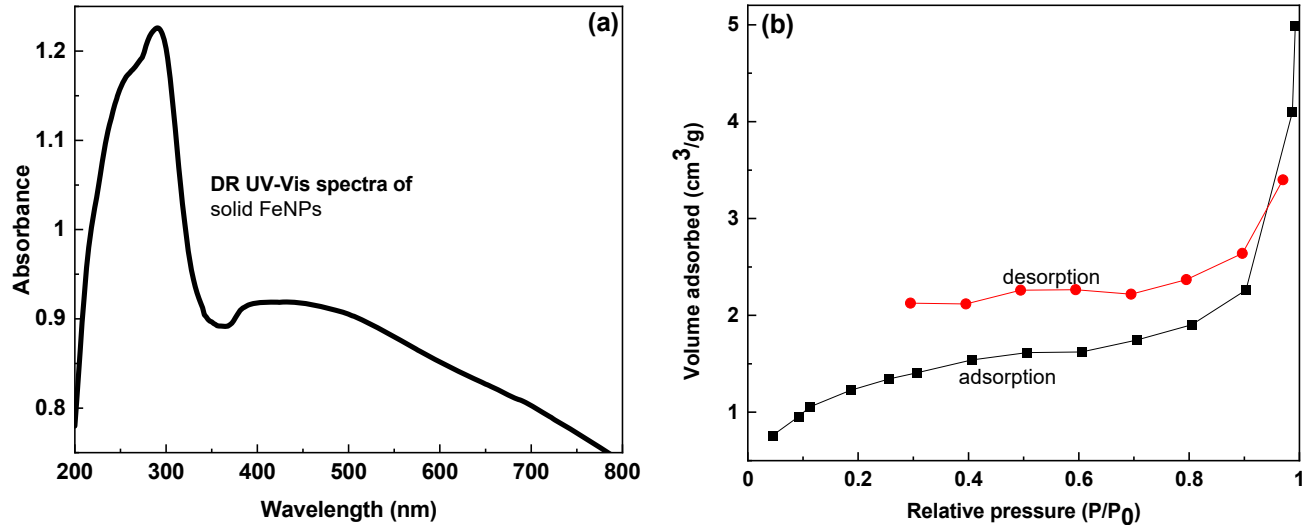

Fig. 7. (a) DR UV-Vis spectra and (b) BET N_2-adsorption-desorption isotherm of solid FeNPs.

Since the plot of ln (C_0/C_t) vs. t (time) gives a linear fit, the slope is taken as the rate constant (k) of reaction. The values of slope (k) were 7.82×10^{-3} min^{-1}in sunlight and 1.5×10^{-2} min^{-1} in UV light. R^2 values were 0.978 in sunlight and 0.934 in UV light. The initial pH of RB (5 ppm) was 5.72 and it was decreased to 3.15 in photocatalytic reactor. Initial pH of RB (20 ppm) was 6.1 and it was decreased to 4.3 at the end of reaction in sunlight.

3.2.1. Mechanism of RB degradation

The FeNPs are known to exhibit high adsorption due to minute dimensions and bulky specific surface area. Also, they are known for reducing ability and activity. The FeNPs act as moderate reducing agents to react with dissolved oxygen (DO) and degrade the contaminants in aqueous medium. The DO may create hydroxyl free radicals, which are highly oxidising to degrade organic pollutants like dyes, phenols, halogenated organic compounds, nitroaromatic compounds etc. [52-53]. In this process, Fe^0 (zero-valent) is converted into Fe^{2+} (divalent) and Fe^{3+} (trivalent) after oxidation with RB dye [53-55].

$Fe^0 + 2H^+ + O_2 \rightarrow Fe^{2+} + H_2O_2$

$Fe^0 + H_2O_2 + 2H^+ \rightarrow Fe^{2+} + 2H_2O$

$Fe^{2+} + H_2O_2 \rightarrow Fe^{3+} + \cdot OH + OH^-$

$^{\bullet}OH + RB \rightarrow$ degraded products

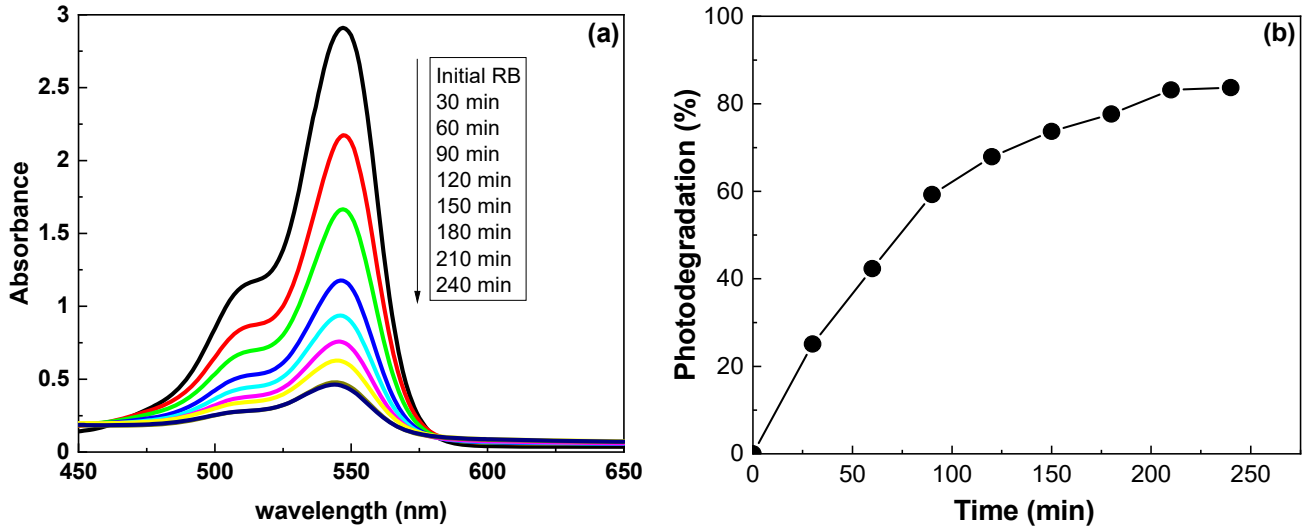

Fig. 8. (a) UV-Vis spectra of RB (20 ppm) with S/L = 0.1g /L in sunlight after irradiation to different time and (b) shows % degradation of RB with irradiation time.

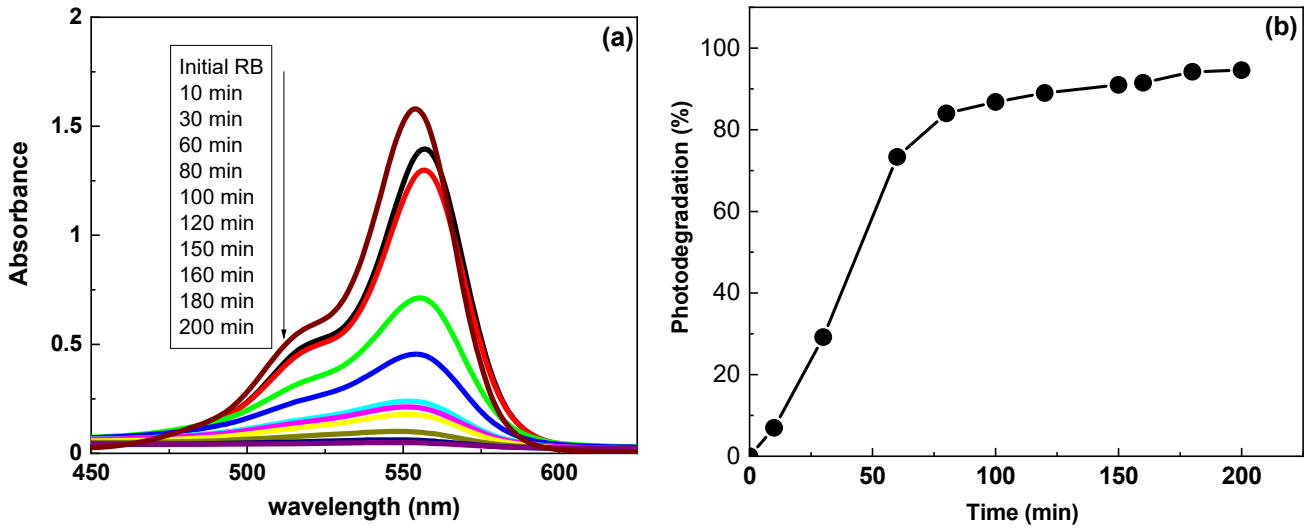

Fig. 9. (a) UV-Vis spectra of RB (5 ppm) with S/L = 0.1g/L irradiated in photocatalytic reactor having UV light 250 W and (b) shows % degradation of RB with time.

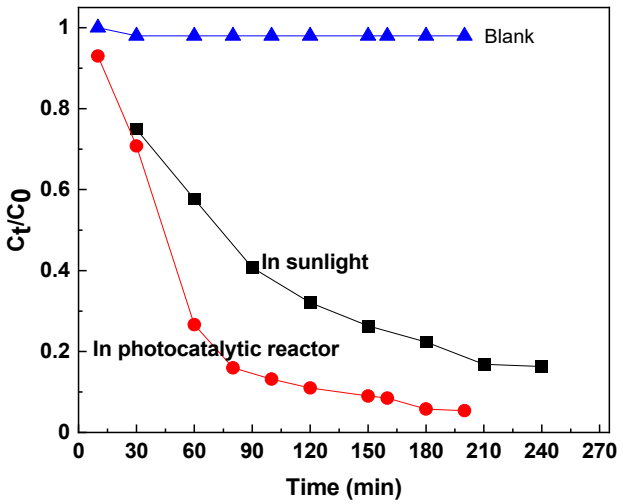

Fig. 10. Plot of C_t/C_0 vs. irradiation time in absence and presence of FeNPs under sunlight and UV light.

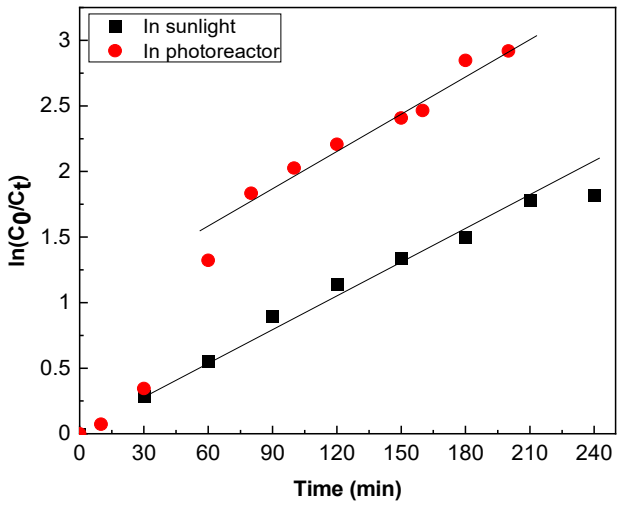

Fig. 11. Plot of ln (C_0/C_t) *vs.* irradiation time for photodegradation of RB by FeNPs.

3.2.2. Degradation product of RB dye

Liquid chromatography mass spectroscopy (LC-MS) was used to confirm degradation of dye and analysis of degraded products. Here LC-MS technique was used to analyse degraded products of RB. The fragmented products were identified by mass fragmentation model as shown in Fig. 12. The prominent peak of standard rose bengal is at m/z 1017. After photodegradation, the RB standard peak almost left and new by-products are observed, having different m/z values. Sinha and Ahmaruzzaman (2016), Bhattacharjee et al (2017) and Farooq et al (2019) have been reported LC-MS degraded products [3, 21, 56]. From m/z values degraded products were identified and degradation pathway of RB is suggested in Scheme 1.

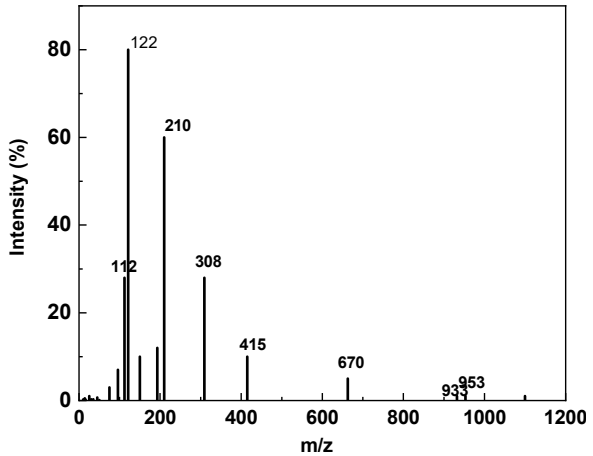

Fig. 12. LCMS result of photodegraded RB (5 ppm of RB + 0.1 g/ L FeNPs).

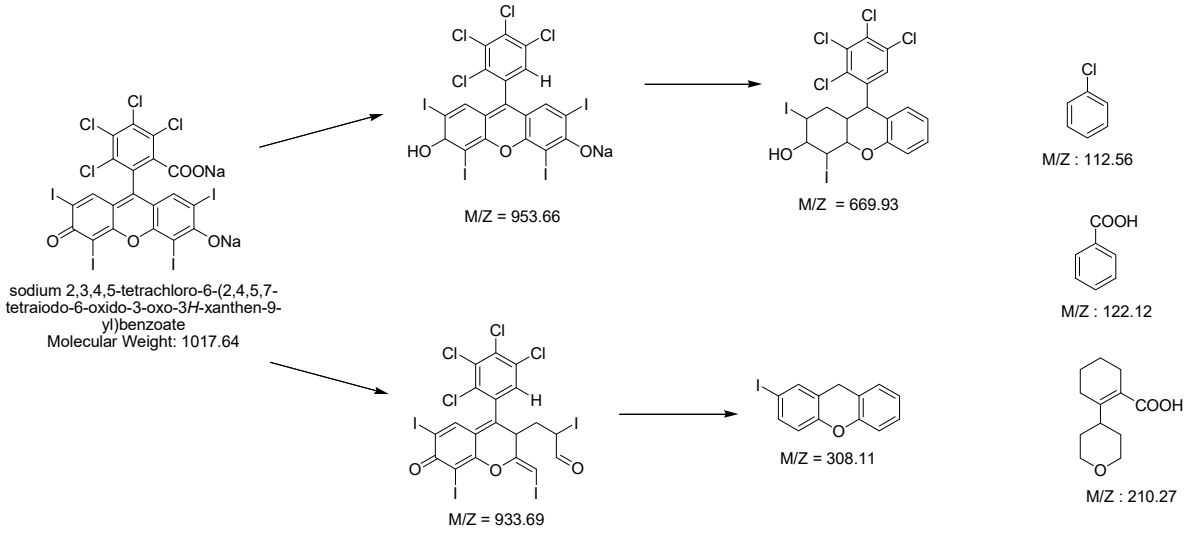

Scheme 1. Possible degradation fragments obtained after photodegradation of rose bengal dye in presence of FeNPs.

4. Conclusions

FeNPs were prepared here by using ferrous nitrate and aqueous *T. arjuna* bark extract in microwave oven. The formation of FeNPs was confirmed from UV-Vis spectra, FT-IR, XRD and FE-SEM analysis. The FeNPs were used to degrade the dye, rose Bengal (RB) from aqueous solution. Based on the UV-Vis spectral analysis, the photodegradation of RB was about 83 % (240 min) in sunlight and 95 % (200 min) in photocatalytic (UV light) reactor. The photodegradation of RB followed the pseudo-first order kinetics. RB is decolorized as it undergoes complete degradation by FeNPs, and LC-MS analysis confirmed the composition of degraded products. Nevertheless, detailed investigation is essential to arrive at the mechanism of RB degradation.

Acknowledgements

Authors gratefully acknowledge the financial support from (i) BRNS/DAE [37 (2)/14/20/2015], Govt. Of India (ii) DST-FIST/ Ministry of Science and Technology [SR/FST/CSI-273/2016], Govt of India and (iii) VGST KFIST Level-II, Dept. of IT, BT and S&T, Govt. of Karnataka, India.

References

[1] S. Yallappa, J. Manjanna, M.A. Sindhe, N.D. Satyanarayan, S.N. Pramod, K. Nagraja, Spectrochim. Acta A 110 (2013) 108-115.
[2] G.E. Hoag, J.B. Collins, J.L. Holcomb, J.R. Hoag, M.N. Nadagouda, R.S. Varma, J. Mater. Chem. 19 (2009) 8671-8677.
[3] T. Sinha, M. Ahmaruzzaman, Photochem. Photobiol. Sci. 15 (2016) 1272-1281.
[4] J. Saha, A. Begum, A. Mukherjee, S. Kumar, Sustain. Environ. Res. 27 (2017) 245-250.
[5] S. Saif, A. Tahir, Y. Chen, Nanomaterials 6 (11) (2016) 209.
[6] M. Ismail, S. Gul, M.I. Khan, M. Khan, A.M. Asiri, S.B. Khan, Green Process. Synth. 8 (2019) 135-143.
[7] D. Raghunandan, S. Basavaraja, B. Mahesh, S. Balaji, S.Y. Manjunath, A. Venkataraman, Nanobiotechnol. 5 (2009) 34-41.
[8] J. Jeyasundari, P.S. Praba, Y.B.A. Jacob, V.S. Vasantha, V. Shanmugaiah, Chem. Sci. Rev. Lett. 22 (2017) 1244-1252.
[9] M. Fazlzadeh, K. Rahmani, A. Zarei, H. Abdoallahzadeh, F. Nasiri, R. Khosravi, Adv. Powder Technol. 28 (2017) 122-130.
[10] T. Wang, X. Jin, Z. Chen, M. Megharaj, R. Naidu, Sci. Total Environ. 466 (2014) 210-213.
[11] M. Amini, B. Pourbadiei, T. Purnima, L. Woo, New J. Chem. 38 (2014) 1250-1255.
[12] H.-Y. Zhu, Y.-Q. Fu, R. Jiang, J.-H. Jiang, L. Xiao, G.-M. Zeng, S.-L. Zhao, Y. Wang, Chem. Eng. J. 173 (2011) 494-502.
[13] R. Wahab, F. Khan, N. Kaushik, J. Musarrat, A. Al-Khedhairy, Sci. Rep. 7 (2017) 42509.
[14] E. N. Zarea, A. Motaharib, M. Sillanpaa, Environ. Res. 162 (2018) 173-195.
[15] S. Karimifard, M. Moghaddam, Sci. Total Environ. 640 (2018) 772-797.
[16] A. Buthiyappan, A.R. Aziz, W. Daud, Rev. Chem. Eng. 32 (2016) 1-47.
[17] Y. Zhou, J. Lu, Y. Zhou, Y. Liu, Environ. Pollut. 252 (2019) 352-365.
[18] H. Guo, Y. Ke, D. Wang, K. Lin, R. Shen, J. Chen, W. Weng, J. Nanopart. Res. 15 (2013) 1475.
[19] L. Laysandra, M.W.M.K. Sari, F.E. Soetaredjo, K. Foe, J.N. Putro, A. Kurniawan, Yi-H. Ju, S. Ismadji, Heliyon 3 (2017) e00488.

[20] M. Vinuth, H.B. Naik, B. Vinoda, S. Pradeepa, G.A. Kumar, K. Chandrashekhar, J. Environ. Anal. Toxicol. 6 (2016) 2-7.
[21] A. Bhattacharjee, M. Ahmaruzzaman, J. Photochem. Photobiol. A 353 (2018) 215-228.
[22] M. Farbod, M. Khademalrasool, Powder Technol. 214 (2011) 344-348.
[23] S. Tuprakay, W. Liengcharernsit, J. Hazard. Mater. B 124 (2005) 53-58.
[24] H. Donga, G. Chena, J. Suna, C. Li, Y. Yua, D. Chen, Appl. Catal. B 134 (2013) 46-54.
[25] Z.W. Seh, S. Liu, M. Low, S.-Y. Zhang, Z. Liu, A. Mlayah, M.-Y. Han, Adv. Mater. 24 (2012) 2310-2314.
[26] J. Lee, D.C. Sorescu, X. Deng, J. Am. Chem. Soc. 133 (2011) 10066-10069.
[27] N. Arabpour, A. Nezamzadeh-Ejhieh, Mater. Sci. Semicond. Process. 31 (2015) 684-692.
[28] Q. Xu, L. Zhang, J. Yu, S. Wageh, A.A. Al-Ghamdi, M. Jaroniec, Mater. Today 21 (2018) 1042-1063.
[29] N. Rahman, Z. Abedin, M.A. Hossain, Am. J. Environ. Sci. 10 (2014) 157-163.
[30] D.W. Elliott, H-L. Lien, W-X. Zhang, J. Environ. Eng.·135 (2009) 317-324.
[31] T. Shahwan, S.A. Sirriah, M. Nairat, E. Boyac, A.E. Eroglu, T.B. Scott, K.R. Hallam, Chem. Eng. J. 172 (2011) 258-266.
[32] M.N. Nadagouda, T.F. Speth, R.S. Varma, Acc. Chem. Res. 44 (2011) 469-478.
[33] S. Joseph, B. Mathew, Spectrochim. Acta A 136 (2015)1371-1379.
[34] K. Patel, S. Kapoor, D.P. Dave, T. Mukherjee, J. Chem. Sci. 117 (1) (2005) 53-60.
[35] T. Ghodselahi, M.A. Vesaghi, A. Shafiekhani, J. Phys. D: Appl. Phys. 42 (2009) 015308.
[36] C. Krishnaraj, E.G. Jagan, S. Rajasekar, P. Selvakumar, P.T. Kalaichelvan, N. Mohan, Colloids Surf. B 76 (2010) 50-56.
[37] V. Subramaniyam, S.R. Subashchandrabose, P. Thavamani, M. Megharaj, Z. Chen, R. Naidu, J. Appl. Phycol. 27 (2015) 1861-1869.
[38] R. Singh, V. Misra, R.P. Singh, J. Nanopart. Res. 13 (2011). 4063-4073.
[39] S. Bansod, M. Rai, World J. Medical Sci. 3 (2008) 81-88.
[40] B. Sultana, F. Anwar, R. Przybylski, Food Chem. 104 (2007) 1106-1114.
[41] S. Jain, P.P. Yadav, V. Gill, N. Vasudeva, N. Singla, Phytochem. Rev. 8 (2009) 491-502.
[42] V. Madhavi, T.N.V.K.V. Prasad, A.V.B. Reddy, B.R. Reddy, G. Madhavi, Spectrochim. Acta A 116 (2013) 17-25.
[43] A. Alshehri, M.A. Malik, Z. Khan, S.A. Al-Thabaiti, N. Hasan, RSC Adv. 7 (2017) 25149-25159.
[44] T. Wang, J. Lin, Z. Chen, M. Megharaj, R. Naidu, J. Clean. Prod. 83 (2014) 413-419.
[45] V. Smuleac, R. Varma, S. Sikdar, D. Bhattacharyy, J. Membrane Sci. 379 (2011) 131-137.
[46] K.M. Kumar, B.K. Mandal, K.S. Kumar, P.S. Reddy, B. Sreedhar, Spectrochim. Acta A 102 (2013) 128-133.
[47] E.C. Njagi, H. Haung, L. Stafford, H. Genuino, H.M. Galindo, J.B. Collins, G.E. Hoag, S.L. Suib, Langmuir 27 (2011) 264-271.
[48] E.A. Essien, D. Kava, M.M. Solomon, Chem. Eng. Comm. 205 (2018) 1568-1582.
[49] J. Esmaili-Hafshejani, A. Nezamzadeh-Ejhieh, J. Hazard. Mater. 316 (2016) 194-203.
[50] S. Jafari, A. Nezamzadeh-Ejhieh, J. Colloid Interf. Sci. 490 (2017) 478-487.
[51] Y. Bagbi, A. Sarswat, S. Tiwari, D. Mohan, A. Pandey, P.R. Solanki, Environ. Nanotechnol. Monit. Manage. 7 (2017) 34-35.
[52] W. Zhang, J. Nanopart. Res. 5 (2003) 323-332.
[53] H.-J. Lu, J.-K. Wang, S. Ferguson, T. Wang, Y. Bao, H.-X. Hao, Nanoscale 8 (2016) 9962-9975.
[54] Z. Zongshan, L. Jingfu, T. Chao, Z. Qunfang, H. Jingtian, J. Guibin, Sci. China Ser. B 51 (2008) 186-192.
[55] L. Xu, J. Wang, J. Hazard. Mater. 186 (2011) 256-264.
[56] U. Farooq, R. Phul, S.M. Alshehri, J. Ahmed, T. Ahmad, Sci. Rep. 9 (2019) 4488.